

Backgrounds to Higgs Boson Searches from $W\gamma^* \rightarrow l\nu\ell(\ell)$ Asymmetric Internal Conversion

Richard C. Gray¹ Can Kilic^{1,2} Michael Park¹
Sunil Somalwar¹ and Scott Thomas¹

¹*Department of Physics
Rutgers University
Piscataway, NJ 08854*

²*Theory Group, Department of Physics and Texas Cosmology Center
The University of Texas at Austin
Austin, TX 78712*

Abstract

A class of potential backgrounds for Higgs boson searches in the $h \rightarrow WW^{(*)} \rightarrow l\nu\ell'\nu$ channel at both the Tevatron and Large Hadron Collider is presented. Backgrounds from $W\gamma$ production with *external* conversion of the on-shell photon in detector material to an asymmetric electron–positron pair, $\gamma \rightarrow e(e)$, with loss of the trailing electron or positron has been treated adequately in Higgs searches. Here we consider analogous backgrounds from $W\gamma^*$ production with *internal* conversion of the off-shell photon in vacuum to an asymmetric lepton–anti-lepton pair $\gamma^* \rightarrow \ell(\ell)$. While the former process yields almost entirely electrons or positrons, the latter can give electron, positron, muon, and anti-muon backgrounds in roughly equal amounts. We estimate that asymmetric internal conversion backgrounds are comparable to the Higgs boson signal in the standard signal region of phase space. These processes also represent potential backgrounds for new physics searches in same-sign di-lepton channels. Some data driven methods to characterize asymmetric internal conversion backgrounds are suggested.

1 Introduction

The search for the Higgs boson has been the cornerstone of the physics program at modern high energy colliders. The Higgs boson of the Standard Model has well defined production and decay modes that allow for mass dependent searches in a number of channels. One of the key discovery modes at hadron colliders is Higgs boson production by gluon-gluon fusion with decay through two leptonically decaying W -bosons, $gg \rightarrow h \rightarrow WW^{(*)} \rightarrow \ell\nu \ell'\nu$, giving opposite sign di-leptons plus missing energy. The dominant background in this channel comes from electroweak pair production of W -bosons, $q\bar{q} \rightarrow WW \rightarrow \ell\nu \ell'\nu$. This background is substantially larger than the Higgs boson signal. However, the two processes have somewhat different kinematic properties that may be exploited using either cut based or multi-variate techniques. Based on the expected kinematic properties of the signal and dominant di-boson background obtained from simulations, searches in this channel have been carried out at both the Tevatron [1, 2, 3] and Large Hadron Collider (LHC) [4, 5].

In addition to the background from W -boson pair production, there are a number of other important processes that contribute background to the opposite sign di-lepton plus missing energy channel. While smaller than the dominant background, some can be comparable to the Higgs boson signal. Among these are a class of backgrounds arising from direct electroweak production of a W -boson in association with some other object that is mis-reconstructed as a fake lepton. This includes a W -boson produced along with jets, where a jet fakes a lepton, $q'\bar{q} \rightarrow Wj \rightarrow \ell\nu \ell'$. Another in this class is production of a W -boson and photon, with the on-shell photon undergoing an asymmetric external conversion to an electron-positron pair in the electromagnetic field of an atomic nucleus within the detector material, $q'\bar{q} \rightarrow W\gamma \rightarrow \ell\nu e(e)$, where the parentheses indicate the trailing electron or positron. If the conversion is sufficiently asymmetric in momentum, the trailing member of the pair is not reconstructed as an independent object and does not ruin the isolation criteria of the leading one, and the converted photon fakes an electron or positron. These backgrounds are treated in ongoing Higgs boson searches [1–5].

Here we consider a closely related process within this class of backgrounds coming from direct production of a W -boson and virtual off-shell photon that undergoes an internal asymmetric conversion in vacuum to a lepton-anti-lepton pair, $q'\bar{q} \rightarrow W\gamma^* \rightarrow \ell\nu \ell'(\ell')$, where $\ell' = e, \mu, \tau$. Initial and final state virtual photon radiation contributions to this process are shown in Fig. 1, with additional contributions coming from W -boson virtual photon radiation near the production or decay vertex. In a manner similar to the external conversions discussed above, if the momentum sharing of the conversion pair is sufficiently asymmetric, the trailing member is not reconstructed as an independent object and does not ruin the isolation criteria of the leading one, and the internal conversion fakes a lepton

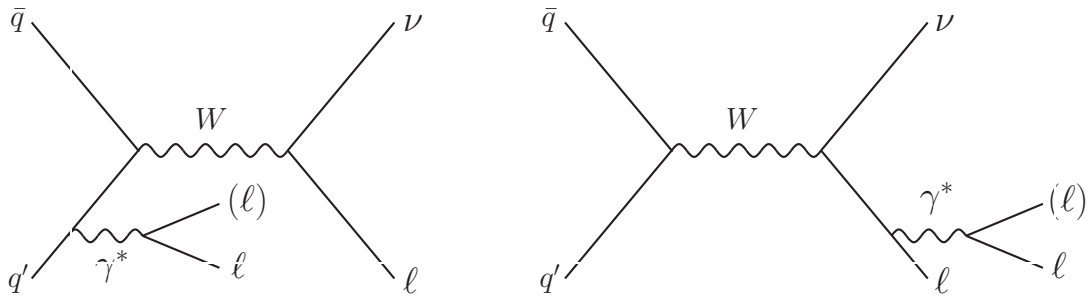


Figure 1: Diagrams for production of a leptonically decaying on/off-shell W -boson at a hadron collider in association with an initial or final state virtual off-shell photon radiation that internally converts in vacuum to a lepton–anti-lepton pair. Parentheses indicate asymmetric internal conversion in which the trailing converted lepton is not reconstructed as an independent isolated object. Diagrams with an off-shell photon radiated from the intermediate W -boson near the production or decay vertex are not shown.

or anti-lepton. This process may be referred to as Loss of a Muon or Electron Following an Asymmetric Internal Conversion (LAME FAIC).

It is instructive to compare and contrast lepton–anti-lepton pairs arising from external and internal conversion. In both cases in order for the conversion to give rise to a single fake object that is reconstructed as a lepton, the conversion must be sufficiently asymmetric as described above. This effective restriction to the asymmetric region of phase space implies that only a fraction of the conversions yield fake lepton objects. Simultaneous reconstruction of a conversion pair with both the lepton and anti-lepton identified could recover most of the remaining symmetric conversion region of the phase space, and possibly give a handle on these backgrounds. Another similarity is that charge conjugation symmetry of electrodynamics ensures that conversion photons yield fake leptons of both charges in roughly equal proportion. This equality may provide a simple but powerful tool for characterizing the kinematic properties and distributions of these backgrounds. It is already used to constrain the total magnitude of backgrounds within this class that arise from a W -boson in association with a mis-reconstructed fake lepton of uncorrelated charge [4, 5].

External and internal conversions differ in important regards. The probability for an on-shell photon to convert in material to a lepton–anti-lepton pair depends strongly on the lepton mass. Near the forward direction in the high energy asymmetric limit, the ratio of external conversion probability for a muon–anti-muon pair to that for an electron–positron pair scales like $\mathcal{P}(\gamma \rightarrow \mu\mu)/\mathcal{P}(\gamma \rightarrow ee) \sim \mathcal{O}(m_e/m_\mu)^2$. So for all practical purposes external conversions give rise only to electron–positron pairs. This is in contrast to internal conversions for which there is only a moderate logarithmic enhancement of electron–positron over muon–anti-muon pairs, as described in the next section. Another key difference is that since external conversion takes place in material, the reconstructed lepton track in this case may emerge part-way through the tracking detector. This feature of missing hits on the inner part of a reconstructed track may be utilized as a criterion for identifying external conversions. It is however not useful for identifying leptons from internal conversion since these originate from the collision vertex.

In the next section, we present the theory of asymmetric internal conversions. Then we study the potential impact of this background on the Higgs search with a simulation. Our simulation of the background at the generator level is done carefully, but the detector simulation that follows is not particularly sophisticated and is only meant to motivate detailed studies by the Higgs search teams. We then conclude with a brief discussion of a possible approach for dealing with the asymmetric internal conversion backgrounds.

2 Asymmetric Internal Conversion

The probability for a photon to split to a lepton–anti-lepton pair by internal conversion may be calculated in the off-shell photon phase space using the optical theorem. The one-loop contribution of a lepton of mass m_ℓ to the discontinuity across the branch cut in the electromagnetic current two-point correlation function gives the conversion probability distribution

$$m_{\ell\ell} \frac{d\mathcal{P}(\gamma^* \rightarrow \ell\ell)}{dm_{\ell\ell}} = \frac{2\alpha}{3\pi} \left(1 - \frac{4m_\ell^2}{m_{\ell\ell}^2}\right)^{1/2} \left(1 + \frac{2m_\ell^2}{m_{\ell\ell}^2}\right) \quad (1)$$

where α is the fine structure constant, and $m_{\ell\ell}$ is the lepton–anti-lepton or equivalently off-shell photon invariant mass. The internal conversion probability has an infrared soft singularity in the lepton–anti-lepton invariant mass phase space that is cutoff only by the lepton mass, $m_{\ell\ell} \geq 2m_\ell$. The probability per logarithmic lepton–anti-lepton invariant mass in the vicinity of the singularity is roughly constant. The total conversion probability integrated between the di-lepton threshold and an ultraviolet matching scale μ is

$$\mathcal{P}(\gamma^* \rightarrow \ell\ell) = \int_{2m_\ell}^{\mu} dm_{\ell\ell} \frac{d\mathcal{P}(\gamma^* \rightarrow \ell\ell)}{dm_{\ell\ell}} = \frac{2\alpha}{3\pi} \left[\ln(\mu/m_\ell) - \frac{5}{6} + \mathcal{O}(m_\ell/\mu)^4 \right] \quad (2)$$

In leading logarithmic approximation, the infrared singular region of the lepton–anti-lepton invariant mass phase space gives the dominant contribution to the process of internal conversion. The contributions from non-singular regions of phase space with $m_{\ell\ell} > \mu$ are formally $\mathcal{O}(1)$ corrections to the logarithm in the brackets in (2). In the background processes of interest here, the total probability for a high energy photon to undergo internal conversion to a lepton–anti-lepton pair is $\mathcal{O}(1\%)$. For example, with $\mu \sim 10$ GeV the splitting probability to an electron–positron pair is $\mathcal{P}(\gamma^* \rightarrow ee) \simeq 1.4 \times 10^{-2}$, to a muon–anti-muon pair is $\mathcal{P}(\gamma^* \rightarrow \mu\mu) \simeq 5.7 \times 10^{-3}$, and to a tau–anti-tau pair is $\mathcal{P}(\gamma^* \rightarrow \tau\tau) \simeq 1.4 \times 10^{-3}$.

An important kinematic property of internal conversion is the degree of asymmetry between the lepton and anti-lepton. In order to characterize this asymmetry it is useful to define the momentum fraction carried by the negatively charged lepton in the direction of motion of the off-shell photon, $z = p_{\ell-}^{\parallel} / (p_{\ell+}^{\parallel} + p_{\ell-}^{\parallel})$. In the high energy co-linear limit in which the lepton–anti-lepton pair emerges in the direction of the off-shell photon, the momentum fraction is related to the lepton decay angle θ in the off-shell photon frame as measured with respect to its direction of motion by $z = \frac{1}{2}(1 + \beta \cos \theta)$, where $\beta = \sqrt{1 - 4m_{\ell}^2/m_{\ell\ell}^2}$ is the lepton velocity in this frame. The momentum fraction in the co-linear limit lies in the range $\frac{1}{2}(1 - \beta) \leq z \leq \frac{1}{2}(1 + \beta)$. The probability distribution with respect to this momentum fraction depends on the polarization of the off-shell photon. In high energy scattering processes the probability for emission of an off-shell photon with longitudinal polarization is suppressed with respect to transverse polarization by $\mathcal{O}(m_{\gamma^*}/M)^2$, where M is an ultraviolet mass scale associated with the hard scattering process. So for the backgrounds of interest here, longitudinal polarization may be neglected.

The normalized probability distribution with respect to the momentum fraction in the co-linear limit for transverse polarization may be calculated in the two-body lepton–anti-lepton phase space using the optical theorem as described above,

$$\frac{1}{\mathcal{P}(\gamma_T^* \rightarrow \ell\ell)} \frac{d\mathcal{P}(\gamma_T^* \rightarrow \ell\ell)}{dz} \equiv f_T(z, \beta) = \frac{2 - \beta^2 + (1 - 2z)^2}{2\beta(1 - \beta^2/3)} \quad (3)$$

Charge conjugation symmetry ensures that this distribution is invariant under $z \rightarrow 1 - z$. Right at threshold, $m_{\ell\ell} = 2m_{\ell}$, the conversion probability is symmetric with $z = \frac{1}{2}$. However, well above threshold, $m_{\ell\ell}^2 \gg m_{\ell}^2$, the transverse conversion normalized probability distribution becomes

$$f_T(z, \beta) = \frac{3}{4} [1 + (1 - 2z)^2] + \mathcal{O}(m_{\ell}/m_{\ell\ell})^2 \quad (4)$$

with z in the range $0 \leq z \leq 1$. In this limit the distribution is maximized for maximally asymmetric momentum fraction, $f_T(0, 1) = f_T(1, 1) = \frac{3}{2}$, and is minimized for symmetric

momentum sharing, $f_T(\frac{1}{2}, 1) = \frac{3}{4}$. The total normalized probability for internal conversion with momentum fraction $z, 1 - z \leq \epsilon$ in the co-linear limit and well above threshold is

$$\xi(\epsilon) \equiv 2 \int_0^\epsilon dz f_T(z, 1) = 3\epsilon - 3\epsilon^2 + 2\epsilon^3 \quad (5)$$

This conversion fraction of course vanishes as $\epsilon \rightarrow 0$, but is not insignificant for moderately small values of asymmetry. For example, the fraction of internal conversions with asymmetry parameter $\epsilon = 0.15$ is $\xi(0.15) \simeq 0.39$. So a sizeable fraction of internal conversions can be fairly asymmetric.

Another important kinematic property of internal conversion is the opening angle between the lepton and anti-lepton. Near the high energy co-linear limit this angle may be written in terms of the lepton momentum fraction and lepton–anti-lepton invariant mass

$$\tan \varphi_{\ell\ell} = \frac{m_{\ell\ell}}{2|\vec{p}_{\ell\ell}|} \frac{\sqrt{\beta^2 - (1 - 2z)^2}}{z(1 - z)} + \mathcal{O}(m_{\ell\ell}^2 / (|\vec{p}_{\ell\ell}| m_\ell))^3 \quad (6)$$

where $|\vec{p}_{\ell\ell}|$ is the laboratory frame total momentum. The opening angle is small for lepton–anti-lepton invariant masses in nearly the entire range $2m_\ell \leq m_{\ell\ell} \lesssim |\vec{p}_{\ell\ell}|$ for conversions not too far from the symmetric limit of $z \sim \frac{1}{2}$. The angle is small for all values of momentum fraction, including near maximal asymmetry $z \sim \frac{1}{2}(1 \pm \beta)$, for invariant masses in the range $2m_\ell \leq m_{\ell\ell} \lesssim \sqrt{m_\ell |\vec{p}_{\ell\ell}|}$.

Before proceeding to an evaluation of the Higgs LAME FAIC background, we extend Eqn. (2). The differential cross section with respect to any kinematic quantities X formed from the four-vectors of the initial and final state particles including the lepton–anti-lepton pair is given by

$$\int_{2m_\ell}^\mu dm_{\ell\ell} \frac{d\sigma}{dm_{\ell\ell} dX} (\text{init} \rightarrow \text{final} + \ell\ell) = \mathcal{P}(\gamma^* \rightarrow \ell\ell) \cdot \frac{d\sigma}{dX} (\text{init} \rightarrow \text{final} + \gamma) \Big|_{p_\gamma = p_{\ell\ell}} + \mathcal{O}(\mu/M)^2 \quad (7)$$

where $\mathcal{P}(\gamma^* \rightarrow \ell\ell)$ is the off-shell photon to lepton–anti-lepton pair conversion probability presented in (2), and M is an ultraviolet mass scale associated with the hard scattering process.

3 Simulating Asymmetric Internal Conversion

In order to maximally capture the phase space of the LAME FAIC asymmetric conversions in a simulation, free parameters in the simulation package must be chosen with due care. In addition, the spatial proximity of the conversion leptons in the tracker can have large impact on the extent of LAME FAIC background. The acceptance thus critically depends on the

detector properties, reconstruction algorithms and kinematic selection criteria. Therefore, the conclusions of the study that we describe below are not rigorously quantitative.

In order to simulate 7 TeV LAME FAIC's, we use Madgraph (V5) [6] to separately generate $\ell\nu_\ell e^+e^-$, $\ell\nu_\ell\mu^+\mu^-$ and $\ell\nu_\ell\tau^+\tau^-$ samples. The Z pole is removed in order not to doublecount the WZ background. A rapidity cut of $|\eta| < 2.5$ was used for all leptons. In each case, the p_T of the hardest and the second hardest ℓ is required to be above 5 GeV. To capture asymmetric conversions maximally, p_T of the third lepton is allowed to be as low as 0.1 GeV and the dilepton invariant mass as low as $2m_{\ell\ell}$. It was necessary to alter the Madgraph source code in order to implement these differential thresholds for the daughter leptons. The generation cross section for the three processes as reported by Madgraph are 3878, 1076 and 228 fb for $\ell = e, \mu$ and τ , respectively. For comparison purposes, we also generated the leptonic decay modes for $gg \rightarrow H$ signal ($m_H = 130 \text{ GeV}, H \rightarrow WW$) and $qq \rightarrow WW$ Pythia [7] samples. The cross section for the Higgs sample was scaled up to the NNLO value [8].

These Madgraph and Pythia samples then underwent a generic LHC detector simulation with the PGS [9] software package. We altered the PGS source code as follows to implement physics object isolation in a manner similar to the way it is done at LHC. An isolation variable is calculated for each photon candidate centered on an ECAL cell n as a fractional sum of the transverse energy deposited in ECAL cells surrounding n within a $\eta - \phi$ radius of $\Delta R = 0.4$

$$\gamma_{\text{iso},n} \equiv \sum_{\substack{\text{ECAL cells} \\ k \neq n}} \frac{E_{T,k} |_{\Delta R < 0.4}}{E_{T,\gamma,n}} \quad (8)$$

Identified photons are required to satisfy $\gamma_{\text{iso},n} < 0.1$. This isolation requirement is a good representation of the full photon identification requirements used by the LHC experiments.

The sum p_T of all tracks with p_T greater than 0.5 GeV within an annulus of inner and outer radius of 0.03 and 0.4 respectively in the $\eta - \phi$ plane must be less than 0.15 of the p_T of the candidate muon.

$$T_{\text{iso},\mu} \equiv \sum_{\substack{\{\text{tracks } i \mid p_{T,i} > 0.5 \text{ GeV}, \\ 0.03 \leq \Delta R_{i\mu} \leq 0.4\}}} \frac{p_{T,i}}{p_{T,\mu}} \quad (9)$$

$$T_{\text{iso},\mu} < 0.15$$

$$E_{\text{iso},e} \equiv \sum_{\substack{\{\text{ECAL cells } k \neq e \mid \\ 3 \times 3 \text{ grid surrounding } e\}}} \frac{E_{T,k}}{E_{T,e}} \quad (10)$$

$$E_{\text{iso},e} < 0.1.$$

$$p_{T,\text{iso},e} \equiv \sum_{\substack{\{\text{tracks } i \mid p_{T,i} > 0.5 \text{ GeV}, \\ \Delta R_{ie} \leq 0.4\}}} p_{T,i} \quad (11)$$

$$p_{T,\text{iso},e} < 5 \text{ GeV}$$

$$\rho_e \equiv \frac{E_{T,\text{ECAL cell } e}}{p_{T,\text{track } e}} \quad (12)$$

$$0.5 \leq \rho_e \leq 1.5$$

The total transverse calorimeter energy in a (3×3) grid¹ around the candidate electron (excluding the candidate cell) is defined as ETISO. PGS then imposes the requirement that $\text{ETISO} / E_t(\text{candidate})$ be less than 10%. The total P_t of tracks with $P_t > 0.5$ GeV within a $\Delta R < 0.40$ cone is defined as PTISO. In this case, this excludes the leading electron track. It must satisfy: $\text{PTISO} < 5$ GeV. Finally the ratio of the calorimeter cell energy to the Pt of the candidate track, E/P, should be within 50% to 150%.

Armed with the LAME FAIC event generation followed by a rudimentary detector simulation, now are in a position to evaluate the Higgs background.

4 Di-lepton Plus Missing Energy Background from Asymmetric Internal Conversion

We apply a set of selection criteria (“WW Analysis”) that mimic typical WW selection criteria. These get the data sample ready for final kinematic selection and discrimination between the signal and the background (“Higgs Analysis”). Table 1 lists these selection criteria.

Figs 2, 3, and 4 show distributions of some of the standard kinematics variables used in Higgs searches. The W^+W^- analysis selection given in Table 1 are used for each of the three processes. In Fig. 5, we show the distribution of transverse mass of the leading lepton plus missing energy. This variable is useful for isolating events with a virtual off-shell photon radiated from the initial state or the W -boson near the production vertex. This is to be contrasted with the transverse mass of the both leptons plus missing energy shown in Fig 4., which is useful for isolating events with a virtual off-shell photon radiated from the final state lepton or the W -boson near the decay vertex. It is seen from these figures that at the W^+W^- selection level, the overall kinematic features of the LAME FAIC background resemble those of the Higgs rather than those of the WW background. While the azimuthal angle distribution is very similar for LAME FAIC’s and the Higgs, the mass distributions

¹We used an ECAL cell size in η and ϕ of 0.087, the default value in the PGS parameter set for CMS.

	$ee + \mu\mu$	$e\mu$
<u>WW Analysis</u>		
$ \eta_e , \eta_j $	$< 2.5, < 5$	
$\Delta R_{\ell\ell}$	> 0.4	
p_{T_e}	$> 10 \text{ GeV}$	
p_{T_μ}	$> 3 \text{ GeV}$	
p_{T_j}	$> 30 \text{ GeV}$	
$p_{T_{\ell_1}}, p_{T_{\ell_2}}$	$> 20, 10 \text{ GeV}$	
N_ℓ, N_j	Exactly (2,0)	
$Q_{\ell_1} Q_{\ell_2}$	-1	
$\cancel{E}_T^{\text{proj}}$	$> 40 \text{ GeV}$	$> 20 \text{ GeV}$
$m_{\ell\ell}$	$> 12 \text{ GeV}$	-
$ m_{\ell\ell} - m_Z $	$> 15 \text{ GeV}$	-
<u>Higgs Analysis</u>		
$m_{\ell\ell}$	$< 50 \text{ GeV}$	
$\Delta\phi_{\ell\ell}$	$< \pi/2$	
$m_{T,\ell\ell\cancel{E}_T}$	90 – 130 GeV	

Table 1: Selection criteria and requirements for a representative opposite sign di-lepton plus missing energy W^+W^- analysis, along with additional requirements for a representative 130 GeV Higgs analysis. Jets are defined with a cone algorithm with $\Delta R = 0.5$. The projected missing transverse energy is defined to be the missing transverse energy, $\cancel{E}_T^{\text{proj}} = \cancel{E}_T$ if $\Delta\phi_{\min} > \pi/2$, and to be $\cancel{E}_T^{\text{proj}} = \cancel{E}_T \sin(\Delta\phi_{\min})$ if $\Delta\phi_{\min} < \pi/2$, where $\Delta\phi_{\min} = \min\{\Delta\phi_{\ell_1\cancel{E}_T}, \Delta\phi_{\ell_2\cancel{E}_T}\}$.

differ since the former peaks at a lower mass. Dilepton yields for various samples are

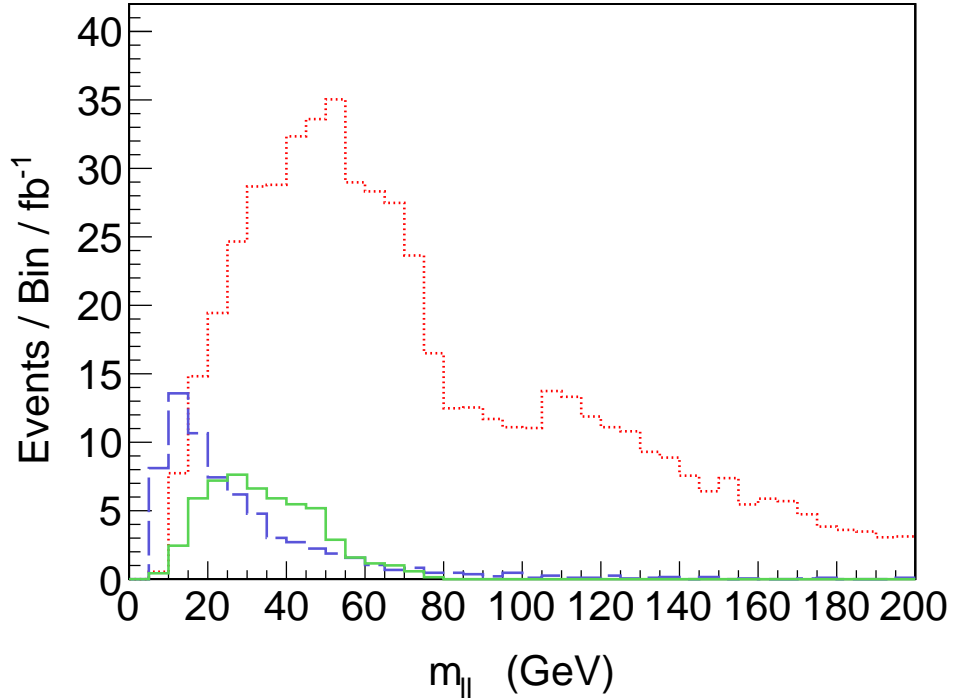


Figure 2: Di-lepton invariant mass distributions arising from pp collisions at 7 TeV for the W^+W^- analysis selection and requirements given in Table 1 with PGS acceptance for the processes $q\bar{q}' \rightarrow W^+W^- \rightarrow \ell^+\nu \ell'^-\bar{\nu}$ (red dotted), $q\bar{q}' \rightarrow W^\pm\gamma^* \rightarrow \ell^\pm\nu \ell'^\mp(\ell'^\pm)$ (blue dashed), and $gg \rightarrow h \rightarrow W^+W^- \rightarrow \ell^+\nu \ell'^-\bar{\nu}$ (green solid) with a Higgs boson mass of 130 GeV. The leptons $\ell, \ell' = e, \mu$, and ν refers to both neutrinos and anti-neutrinos. The distributions are overlaid, not stacked, with 5 GeV bins.

shown in Table 2. The first three rows show the LAME FAIC yields for each (lost) lepton flavor. The relative flavor decomposition in the table could be inexact due to the limitations in simulating detector acceptance of an asymmetric conversion pair. The fourth row shows the total yield for the LAME FAIC events. The last two rows show the same for 130 GeV Higgs and WW, respectively. After the WW selection, it is seen that the LAME FAIC yields are comparable to those of the Higgs even if both are significantly smaller than the WW yields. Table 2 also shows dilepton yields after the Higgs selection. As expected from the accompanying kinematic distributions, the WW background is reduced drastically. The LAME FAIC's, however, still pose an $\mathcal{O}(20\%)$ background to the 130 GeV Higgs signal.

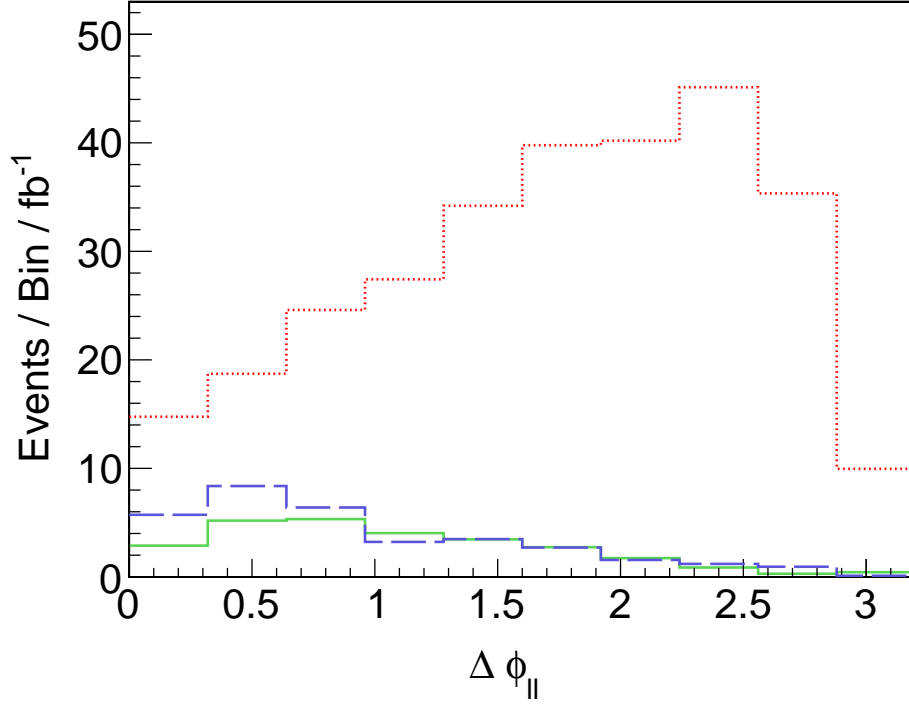


Figure 3: Di-lepton azimuthal angle difference distributions arising from pp collisions at 7 TeV for the W^+W^- analysis selection and requirements given in Table 1 with PGS acceptance for the processes $q\bar{q}' \rightarrow W^+W^- \rightarrow \ell^+\nu \ell'^-\bar{\nu}$ (red dotted), $q\bar{q}' \rightarrow W^\pm\gamma^* \rightarrow \ell^\pm\nu \ell'^\mp(\ell'^\pm)$ (blue dashed), and $gg \rightarrow h \rightarrow W^+W^- \rightarrow \ell^+\nu \ell'^-\bar{\nu}$ (green solid) with a Higgs boson mass of 130 GeV. The leptons $\ell, \ell' = e, \mu$, and ν refers to both neutrinos and anti-neutrinos. The distributions are overlaid, not stacked, with bins of size $\pi/10$ radians.

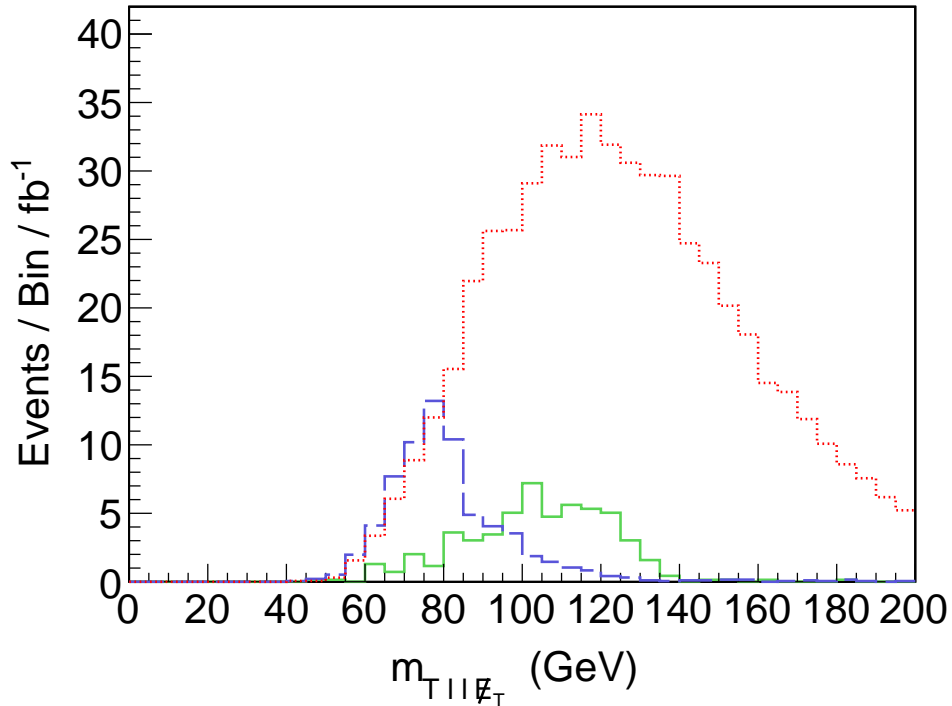


Figure 4: Di-lepton plus missing energy transverse mass distributions arising from pp collisions at 7 TeV for the W^+W^- analysis selection and requirements given in Table 1 with PGS acceptance for the processes $q\bar{q}' \rightarrow W^+W^- \rightarrow \ell^+\nu \ell'^-\bar{\nu}$ (red dotted), $q\bar{q}' \rightarrow W^\pm\gamma^* \rightarrow \ell^\pm\nu \ell'^\mp(\ell'^\pm)$ (blue dashed), and $gg \rightarrow h \rightarrow W^+W^- \rightarrow \ell^+\nu \ell'^-\bar{\nu}$ (green solid) with a Higgs boson mass of 130 GeV. The leptons $\ell, \ell' = e, \mu$, and ν refers to both neutrinos and anti-neutrinos. The distributions are overlaid, not stacked with 5 GeV bins.

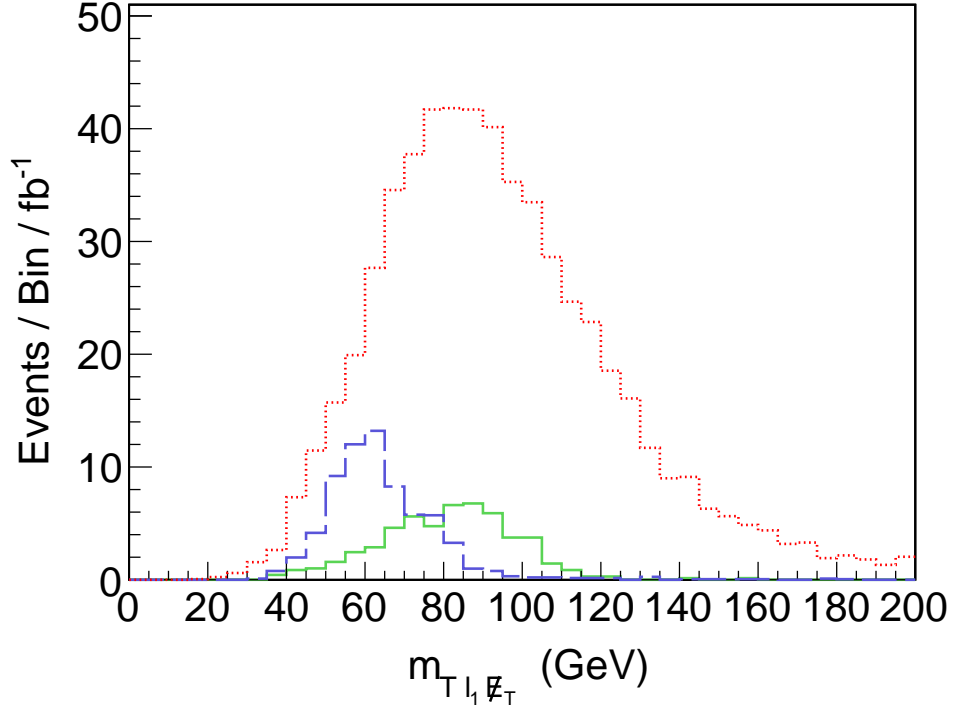


Figure 5: Transverse mass of the leading lepton plus missing energy distributions arising from pp collisions at 7 TeV for the W^+W^- analysis selection and requirements given in Table 1 with PGS acceptance for the processes $q\bar{q}' \rightarrow W^+W^- \rightarrow \ell^+\nu \ell'^-\bar{\nu}$ (red dotted), $q\bar{q}' \rightarrow W^\pm\gamma^* \rightarrow \ell^\pm\nu \ell'^\mp(\ell'^\pm)$ (blue dashed), and $gg \rightarrow h \rightarrow W^+W^- \rightarrow \ell^+\nu \ell'^-\bar{\nu}$ (green solid) with a Higgs boson mass of 130 GeV. The leptons $\ell, \ell' = e, \mu$, and ν refers to both neutrinos and anti-neutrinos. The distributions are overlaid, not stacked with 5 GeV bins.

	$\sigma \cdot \text{Br} \cdot \mathcal{A}_{\text{PGS}}$ (fb)					
	W^+W^- Analysis			Higgs Analysis		
	e^+e^-	$e^\pm\mu^\mp$	$\mu^+\mu^-$	e^+e^-	$e^\pm\mu^\mp$	$\mu^+\mu^-$
$q\bar{q}' \rightarrow W^\pm\gamma^* \rightarrow \ell^\pm\nu e^\mp(e^\pm)$	7.7	47	0	2.2	3.5	0
$q\bar{q}' \rightarrow W^\pm\gamma^* \rightarrow \ell^\pm\nu \mu^\mp(\mu^\pm)$	0	9.9	3.4	0	0.3	1.0
$q\bar{q}' \rightarrow W^\pm\gamma^* \rightarrow \ell^\pm\nu \tau^\mp(\tau^\pm)$	< 0.1	0.4	< 0.1	< 0.1	< 0.1	< 0.1
$q\bar{q}' \rightarrow W^\pm\gamma^* \rightarrow \ell^\pm\nu \ell'^\mp(\ell'^\pm)$	7.7	57	3.4	2.2	3.8	1.0
$gg \rightarrow h \rightarrow W^+W^- \rightarrow \ell^+\nu \ell'^-\nu$	9.4	33	13	7.2	16	9.4
$q\bar{q} \rightarrow W^+W^- \rightarrow \ell^+\nu \ell'^-\nu$	90	390	105	21	47	21

Table 2: Cross sections times branching ratios times PGS acceptance in fb resulting from pp collisions at 7 TeV in the e^+e^- , $e^\pm\mu^\mp$, and $\mu^+\mu^-$ channels for various processes contributing to the W^+W^- and Higgs analyses given in Table 1. The asymmetric internal conversion processes do not include any Z boson contributions. The penultimate process includes only gluon fusion production of a 130 GeV Higgs boson, while the final process does not include any Higgs boson contributions. The leptons $\ell, \ell' = e, \mu$, and ν refers to both neutrinos and anti-neutrinos. Parentheses indicate that the lepton is not reconstructed as an independent isolated object.

5 Concluding Remarks

We have shown that the internal conversion background is potentially sizeable and is sufficiently similar in kinematics to the Higgs signal that it could throw a wrench in the delicate workings of sophisticated multivariate analysis techniques employed in the Higgs searches. Similarities between internal conversions and Higgs in both yield and kinematic properties warrants experimental studies of this background. Furthermore, even sophisticated simulation may prove inadequate in quantifying detector acceptance of the surviving lepton since the impact of the lost low- p_T lepton on the tracking and isolation of the surviving one is difficult to gauge. In that case, and for the purposes of making searches robust, it behooves the Higgs hunters to employ data-based techniques for reducing and then incorporating this background into multivariate schemes.

Since the LAME FAIC background should yield equal number of same-sign (SS) and opposite-sign (OS) dileptons, the SS dilepton data sample can be used to constrain the LAME FAIC background in the OS (Higgs) analysis. A detailed understanding of the $t\bar{t}$ bar, electroweak and $W\gamma$ external conversion backgrounds of the SS sample would constrain the OS LAME FAIC's. A Monte Carlo simulation of the OS LAME FAIC's that has been validated with the SS data sample could be integrated in the Higgs multivariate analysis techniques.

To conclude, the opposite-sign dileptons resulting from asymmetric $W\gamma^*$ internal conversion form a potential background for the Higgs searches. This background has not been addressed in the recent results released by the Tevatron or LHC Higgs search teams. While our limited study lacks the quantitative rigor in simulating the intricacies of detector acceptance in the presence of a soft conversion lepton, it is possible that the more detailed simulation tools currently used by the Higgs search teams are also inadequate in addressing it, thus necessitating development of data-based techniques.

Acknowledgments

We would like to thank Johan Alwall, Emmanuel Contreras-Campana, Yuri Gershtein, Amit Lath, Yue Zhao and other colleagues at Rutgers for their insights and constructive comments. The research of CK, MP and ST was supported in part by DOE grant DE-FG02-96ER40959 and NSF Grant PHY-0969020. The research of RG and SS was supported in part by NSF grant PHY-0969282.

References

- [1] T. Aaltonen *et al.* [The CDF Collaboration], “Inclusive Search for Standard Model Higgs Boson Production in the WW Decay Channel using the CDF II Detector,” Phys. Rev. Lett. **104**, 061803 (2010) [arXiv:1001.4468 [hep-ex]].
- [2] V. M. Abazov *et al.* [The D0 Collaboration], “Search for Higgs boson production in dilepton and missing energy final states with 5.4 fb^{-1} of $p\bar{p}$ collisions at $\sqrt{s} = 1.96 \text{ TeV}$,” Phys. Rev. Lett. **104**, 061804 (2010) [arXiv:1001.4481 [hep-ex]].
- [3] T. Aaltonen *et al.* [CDF and D0 Collaborations], “Combination of Tevatron searches for the standard model Higgs boson in the W^+W^- decay mode,” Phys. Rev. Lett. **104**, 061802 (2010) [arXiv:1001.4162 [hep-ex]].
- [4] S. Chatrchyan *et al.* [CMS Collaboration], “Measurement of W^+W^- Production and Search for the Higgs Boson in pp Collisions at $\sqrt{s} = 7 \text{ TeV}$,” Phys. Lett. B **699**, 25 (2011) [arXiv:1102.5429 [hep-ex]].
- [5] G. Aad *et al.* [ATLAS Collaboration], “Limits on the production of the Standard Model Higgs Boson in pp collisions at $\sqrt{s} = 7 \text{ TeV}$ with the ATLAS detector,” arXiv:1106.2748 [hep-ex].
- [6] J. Alwall, M. Herquet, F. Maltoni, O. Mattelaer, T. Stelzer, “MadGraph 5 : Going Beyond,” JHEP **1106**, 128 (2011). [arXiv:1106.0522 [hep-ph]].
- [7] T. Sjostrand, S. Mrenna, and P. Z. Skands, “A Brief Introduction to PYTHIA 8.1”, Comput. Phys. Commun. **178**, 852–867 (2008) [arXiv:0710.3820 [hep-ph]].
- [8] S. Dittmaier *et al.* [LHC Higgs Cross Section Working Group Collaboration], [arXiv:1101.0593 [hep-ph]].
- [9] J. Conway *et al.*, “PGS 4: Pretty Good Simulation of high energy collisions,” 2006, www.physics.ucdavis.edu/~conway/research/software/pgs/pgs4-general.html
- [10] J. M. Campbell, R. K. Ellis, C. Williams, JHEP **1107**, 018 (2011). [arXiv:1105.0020 [hep-ph]].